Journal of Cleaner Production 183 (2018) 1110–1121

Contents lists available at ScienceDirect

Journal of Cleaner Production

journal homepage: www.elsevier.com/locate/jclepro

A high temporal-spatial resolution air pollutant emission inventory for agricultural machinery in China

Jianlei Lang [a, *], Jingjing Tian [a], Ying Zhou [a, **], Kanghong Li [a], Dongsheng Chen [a], Qing Huang [b], Xiaofan Xing [a], Yanyun Zhang [a], Shuiyuan Cheng [a]

[a] Key Laboratory of Beijing on Regional Air Pollution Control, College of Environmental & Energy Engineering, Beijing University of Technology, Beijing, 100124, China
[b] School of Environment, Jinan University, Guangzhou, 510632, China

ARTICLE INFO

Article history:
Received 10 August 2017
Received in revised form
8 January 2018
Accepted 12 February 2018
Available online 22 February 2018

Keywords:
Agricultural machinery emissions
China
County-level
Spatial distribution
Temporal distribution

ABSTRACT

Agricultural machinery is an important non-road mobile source, which can exhaust multi-pollutants, making primary and secondary contributions to the air pollution. China is a significant agricultural country of the world; however, the agricultural machinery emissions research is at an early stage, and an emission inventory with a high temporal-spatial resolution is still needed. In this study, a comprehensive emission inventory with a high temporal-spatial resolution for agricultural machinery in China was first developed. The results showed that the total emissions in 2014 were 262.69 Gg, 249.25 Gg, 1211.39 Gg, 2192.05 Gg, 1448.16 Gg and 25.14 Gg for PM_{10}, $PM_{2.5}$, THC, NOx, CO and SO_2, respectively. Tractors and farm transport vehicles were the top two greatest contributors, accounting for approximately 39.9%-53.6% and 17.4%-24.6%, respectively, of the total emissions of the five pollutants (except THC). The farm transport vehicles contributed the most (81.8%) to the THC emissions. The county-level emissions were further allocated into 1 km × 1 km grids according to source-specific allocation surrogates. The spatial characteristic analysis indicated that high emissions were distributed in northeast, north and central-south China. To obtain a high temporal resolution emission inventory, a comprehensive investigation on the agricultural practice timing in different provinces was conducted. Then, the annual emissions in the different provinces were distributed to a spatial resolution of ten-day periods (i.e. the early, mid- and late ten-day periods in each month). It was found that higher emissions in China occurred in late April, mid-June and early October. In addition, the emission uncertainty was also analyzed based on the Monte Carlo simulation. The estimated high temporal-spatial resolution emission inventory could provide important basic information for environmental/climate implications research, emission control policy making, and air quality modeling.

1. Introduction

Mobile sources can exhaust many kinds of pollutants (e.g., sulfur dioxide (SO_2), nitrogen oxides (NOx), total hydrocarbons (THC), carbon monoxide (CO) and particulate matter (PM)) during the process of fuel combustion. These pollutants can cause direct or indirect adverse influences to air pollution (Gu and Yim, 2016; Liu et al., 2017a; Zhang et al., 2017), human health (Fu and Tai, 2015; Liu et al., 2016; Xie et al., 2016) and climate change (Anenberg et al., 2013; Kapadia et al., 2016; Kodros et al., 2015). For example, emitted PM could directly increase atmospheric particulate matter with a diameter below 2.5 μm ($PM_{2.5}$) concentrations; as important fine particle precursors, SO_2 and NOx can transform into sulfate and nitrate, making a secondary contribution to the $PM_{2.5}$ (Lang et al., 2017; Wu et al., 2016). As a result, the mobile sources are important potential contributors to serious $PM_{2.5}$ pollution levels in China. In fact, the on-road vehicle emissions have drawn much attention in China (He et al., 2016; Liu et al., 2017b). However, non-road mobile sources, especially agricultural machinery emissions, have been given much less attention. China is a significant agricultural country in the world, accounting for 7% of the world's total cultivated land. The number of agricultural employees was 219

* Corresponding author. College of Environmental & Energy Engineering, Key Laboratory of Beijing on Regional Air Pollution Control, Beijing University of Technology, Beijing, 100124, China.
** Corresponding author.
E-mail addresses: jllang@bjut.edu.cn (J. Lang), y.zhou@bjut.edu.cn (Y. Zhou).

https://doi.org/10.1016/j.jclepro.2018.02.120
0959-6526/

million in 2015, second only to the population of China, India, the United States and Indonesia (NBSC, 2015a). Consequently, given the potential contribution to air pollution and considering the amount of Chinese agriculture, it is of great necessity to estimate the pollutant emissions of agricultural machinery to provide basic information for the further study of their environmental implications and for making effective emission mitigation measures.

A few studies have been conducted on agricultural machinery emissions. For example, Wang et al. (2016) established a non-road emission inventory of China in 2012 and found that agricultural machinery contributed the greatest amount of emissions. Zhang et al. (2010) developed a non-road mobile source emission inventory for the Pearl River Delta Region. The SO_2, NOx, volatile organic compounds (VOC), CO and particulate matter with a diameter below 10 μm (PM_{10}) emissions of agricultural machinery accounted for 1.0%, 9.1%, 33.6%, 18.0% and 15.4% of the total non-road emissions in the study, respectively. Ning and Li (2016) estimated the total emissions of mobile sources from 2000 to 2012 in China, indicating that agricultural machinery was the primary emission source, with a contribution ratio of 81%. Fan et al. (2011) calculated the emissions of agricultural machinery for the year 2007 in Beijing by using the fuel consumption-based approach. Based on the fuel consumption, Jin et al. (2014) calculated NOx and PM emissions of agricultural machinery in Tianjin in 2010. It can be found from previous studies that agricultural machinery was indeed an important non-road mobile source, and it was worth further study. However, most of the studies focused on a specific region. The spatial resolution of the emissions was at the country level or province-level. The temporal characteristics of agricultural machinery emissions rarely have been discussed. These cannot satisfy the demand for refining environmental management or the requirements of the model simulation (e.g., CMAQ or CAMx) (Huang et al., 2012a). More studies of fine emission inventory (e.g., at the county level) are required.

As a result, the purpose of this study is to first develop a comprehensive emission inventory with a high temporal (ten-day) and spatial (county level and 1 km) resolution for agricultural machinery in China. In this study, we considered most of the agricultural machinery types of China and six typical pollutants, including PM_{10}, $PM_{2.5}$, THC, NOx, CO and SO_2, based on the year of 2014. A county-level emission inventory was first calculated based on pollutant- and source-specific methods, and then it was allocated to 1 km × 1 km grids according to the source-specific allocation surrogates. The annual emissions in the different provinces were further distributed to the temporal resolution of ten-day periods, based on a comprehensive investigation of the timing diagram of the agricultural practices in the different provinces of mainland China. In addition, the uncertainty of the estimated emissions was also analyzed by the Monto Carlo simulation and a comparison with previous studies.

2. Methodology

2.1. Classification of agricultural machinery

The classification of agricultural machinery was an important basis for developing the emission inventory. In this study, a two-level classification system was established (Table 1), based on the classification standards of the agricultural industry in China (NBSC, 2015b). The first category consists of eight types, which was classified by the main application in agriculture. The tractors, planting machinery and farm transport vehicles were further divided into three, six and three sub-categories, respectively, based on their different powers or usages.

2.2. Emissions calculation

In this study, three kinds of methods were applied to the emission calculation for the different pollutants and various agricultural types. They are presented in the following sub-sections.

2.2.1. Calculation of SO_2 emission

The SO_2 emission was estimated based on the mass balance algorithm, as shown in Eq. (1):

Table 1
The annual average working hours and emission factors for different agricultural machinery.

Category	Sub-category	Average working hours (h)	Emission factors (g/km for Farm transport vehicles, g/kwh for others)				
			PM_{10}	$PM_{2.5}$	THC	NO_x	CO
Tractor							
	Large tractor (L-tractor)	500[a]	1	0.95	1.3	10.5	6.5
	Medium tractor (M-tractor)	500[a]	1.2	1.14	1.3	10.5	6.5
	Small tractor (S-tractor)	500[a]	1.2	1.14	1.3	10.5	6.5
Planting machinery							
	Tilling and machine	380[a]	1.2	1.14	1.3	10.5	6.5
	Machinery for planting and distributing fertilizer	380[a]	1.2	1.14	1.3	10.5	6.5
	Agricultural drainage and irrigation machinery	380[a]	1.2	1.14	1.3	10.5	6.5
	Field managing machine	127[b]	1.2	1.14	1.3	10.5	6.5
	Harvesting machine	150[b]	1.2	1.14	1.3	10.5	6.5
	Post-harvest processing machine	380[a]	1.2	1.14	1.3	10.5	6.5
Farm and sideline products primary processing machinery		380[a]	1.2	1.14	1.3	10.5	6.5
Animal husbandry machinery		722[b]	1.2	1.14	1.3	10.5	6.5
Fishery machinery		73[b]	1.2	1.14	1.3	10.5	6.5
Timber and fruits machinery		103[b]	1.2	1.14	1.3	10.5	6.5
Farmland capital construction machinery		380[a]	1	0.95	1.3	10.5	6.5
Farm transport vehicle							
	Three-wheeled transport vehicle		0.18	0.17	2.85	1.1	0.96
	Low-speed truck		0.19	0.18	2.85	1.1	0.89
	Hand-hole modified vehicle		0.18	0.17	2.85	1.1	0.96

[a] MEP, 2014.
[b] Fan et al., 2011.

$$E_{i,j} = FC_{i,j} \times S_i \times \frac{M_{SO2}}{M_S} \times 10^{-9} \quad (1)$$

where $E_{i,j}$ is the SO_2 emission (Mg) of the agricultural machinery j in region i; FC is the annual fuel consumption (kg), which is described in section 2.3; S_i is the sulfur content of the fuel (diesel) - in the year of 2014, it was 10 mg/kg in Beijing, 50 mg/kg in Shanghai and Guangzhou, and 350 mg/kg in other provinces of mainland China, respectively (Lang et al., 2016); M_{SO2} (64) and M_S (32) are the formula weight of SO_2 and S, respectively.

2.2.2. Calculation of the agricultural transporter emission

The emission calculation method for the agricultural transport vehicles is similar to that for the on-road vehicles, as shown in Eq. (2):

$$E_{i,k} = \sum_j \left(P_{i,j} \times KT_j \times EF_{j,k} \right) \times 10^{-6} \quad (2)$$

where $E_{i,k}$ represents the emission (Mg) of the pollutant k in region i; $P_{i,j}$ is the population of the agricultural transport vehicle j in region i; KT is the average annual kilometers travelled (km) of the agricultural transport vehicle - it is 23,000 km, 30,900 km and 23,000 km for a three-wheeled transport vehicle, low-speed truck and hand-hole modified vehicle, respectively (MEP, 2014); EF is the emission factor (g/km). The pollutants (k) include PM_{10}, $PM_{2.5}$, THC, NO_x and CO; the population (P) and the emission factor (EF) are described in section 2.3.

2.2.3. Calculation of agricultural machinery emission

The engine power-based approach was used to calculate the emission of agricultural machinery, except for agricultural transport vehicles, as shown in Eq. (3):

$$E_{i,k} = \sum_j \left(P_j \times G_{i,j} \times LF_j \times T_j \times EF_{j,k} \right) \times 10^{-6} \quad (3)$$

where $E_{i,k}$ is the total emission (Mg) of the pollutant k in region i; P_j is the population of the agricultural machinery j; G is the average installed engine power (kw); LF is the load factor (0.65) (MEP, 2014); T is the average agricultural machinery activity time (h) in one year; EF is the corresponding emission factor (g/kwh). The pollutants (k) include PM_{10}, $PM_{2.5}$, THC, NO_x and CO; the activity time (T) was obtained from the technical guidelines and literature (Fan et al., 2011; MEP, 2014), as shown in Table 1; the population (P), average installed engine power (G) and emission factor (EF) and are described in section 2.3.

2.3. Data description

2.3.1. Activity data

(1) County-level population

The county-level population of the agricultural machinery is important basic data for developing a high-resolution emission inventory. However, it cannot be directly obtained from the statistical information of China. We can get the province-level population (Fig. 1 & Fig. S1) and the province- and county-level total power (NBSC, 2015b; NBSC, 2015c). We conducted a correlation analysis between the populations and the total powers of the agricultural machinery, and a good correlation was found ($R > 0.8$). Hence, the county-level population could be obtained by distributing the province-level numbers to each county based on the county-level total power of the agricultural machinery (Zheng et al., 2017).

(2) Average installed engine power

The average installed engine power (AIEP) of the different agricultural machinery was another important parameter for estimating the air pollutants emissions. Normally, the same AIEP was used for the different regions in most of the previous studies. This could cause uncertainties in the calculated emissions, because it cannot reflect the differences of the AIEP in the various provinces. In this study, we collected the provincial population and total power of the various agricultural machineries (NBSC, 2015b) and then calculated the province- and machinery-specific AIEP for 31 municipalities/provinces by dividing the power by the corresponding population. It can be found in Table S1 (in the supplement) that there are obvious differences among the AIEPs of the different provinces. For example, in the case of a three-wheeled transport vehicle, the maximum and minimum AIEP values were 17.54 kw

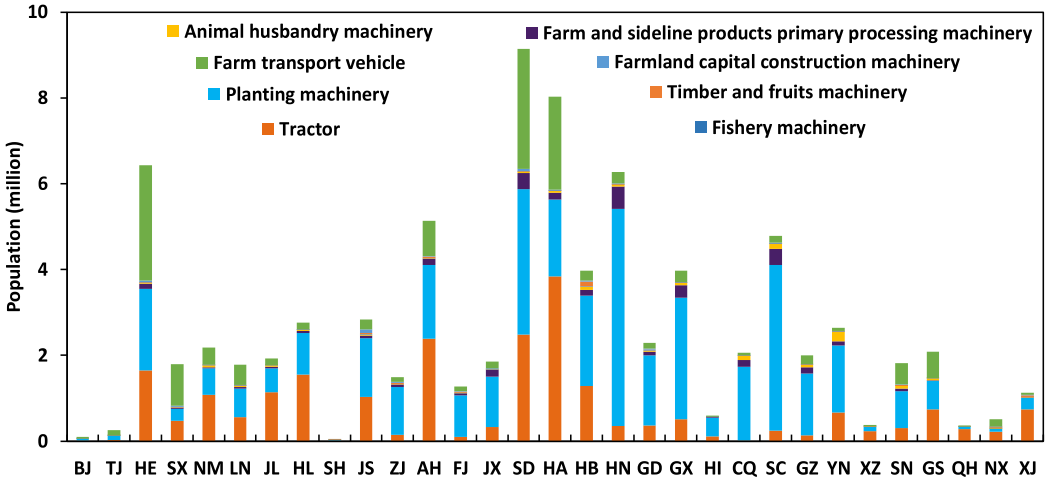

Fig. 1. Population of the agricultural machinery in 31 provinces/municipalities in 2014 (BJ: Beijing, TJ: Tianjin, HE: Hebei, SX: Shanxi, NM: Inner-Mongolia, LN: Liaoning, JL: Jilin, HL: Heilongjiang, SH: Shanghai, JS: Jiangsu, ZJ: Zhejiang, AH: Anhui, FJ: Fujian, JX: Jiangxi, SD: Shandong, HA: Henan, HB: Hubei, HN: Hunan, GD: Guangdong, GX: Guangxi, HI: Hainan, CQ: Chongqing, SC: Sichuan, GZ: Guizhou, YN: Yunnan, XZ: Tibet, SN: Shaanxi, GS: Gansu, QH: Qinghai, NX: Ningxia, XJ: Xinjiang).

and 7.89kw in Chongqing and Zhejiang, respectively. If the mean AIEP of different provinces (12.70 kw) is used for estimating the pollutant emissions, the error would be −27.6% and 61.1% for Chongqing and Zhejiang, respectively. The standard deviation (SD, 1.97 kw) of the AIEP in different provinces was further calculated, accounting for 15.5% (SD/MEAN) of the mean value. The SD/MEAN values for the other agricultural machinery were also estimated (Table S1), and the change range was 7.7%-84.3%, with a mean value of 33.6%. These indicate that the calculation of the province-specific AIEP was necessary, and it could decrease the uncertainty of the emissions to a great extent.

(3) Diesel consumption

The diesel consumption was used for the calculation of the SO_2 emissions. The provincial level sum of the diesel consumption was obtained from the China Agricultural Machinery Industry Yearbook (NBSC, 2015b), which is shown in Table S2 of the supplement. The county-level fuel consumption values were calculated by using the same method used for the county-level population based on the provincial diesel consumption and the county-level total power of the agricultural machinery (Fan et al., 2011; Pan et al., 2015; Wei, 2013).

2.3.2. Emissions factor

The emission factor is also an important parameter for establishing the atmospheric pollutant emission inventory. In this study, the emission factors are referred to as the Non-road Mobile Source Emissions Inventory Compiled Technical Guidelines (MEP, 2014). They are listed in Table 1.

The sources of the data discussed in this section, including the activity data and the emission factors, are summarized in Table S3.

2.4. Spatial distribution

To improve the resolution of the emission inventory and to provide the grid emissions for a model simulation, the emissions of the different counties were allocated into 1 km × 1 km grid cells. GIS (Geographic Information System) software was the main tool for conducting the spatial distribution. Source-specific allocation surrogates were used according to the homologous agricultural machinery characteristics: (1) for tractors, planting machinery, farmland capital construction machinery and farm transport vehicles, we selected croplands land cover to allocate the county emissions to grids; (2) for timber and fruit machinery, forest land cover was the distribution basis; (3) for farm and sideline products, primary processing machinery and animal husbandry machinery, rural population density was the proxy; and (4) for fishery machinery, fisherman density was the allocation surrogate. Croplands land cover and forest land cover were screened from the land use data (MODIS land cover) provided by Ran et al. (2010). The rural population density was obtained from satellite data by intersecting croplands land cover and population. The fisherman density was obtained based on land use cover and population satellite data.

We allocated emissions to a grid by using the following equation:

$$E_i = \frac{X_i}{X_m} \times E_m \tag{4}$$

where E_i is the emission in the ith grid; X_i is the croplands density, forest density, rural population density or fisherman density in the ith grid; X_m is the total croplands density, forest density, rural population density or fisherman density in the county m; and E_m is the total emissions from the tractors, planting machinery, farmland capital construction machinery, farm transport vehicles, timber and fruit machinery, farm, sideline, products primary processing machinery, animal husbandry machinery or fishery machinery in the county m.

2.5. Temporal allocation

To obtain the temporal variation of the agricultural machinery emissions, the ten-day uneven coefficients had to be determined. This study conducted a comprehensive investigation on the timing diagram of the agricultural practices in the different provinces of mainland China, referring to the agricultural practice information (MOA, 2014) and literature (Huang et al., 2012b; Li et al., 2016; Qiu et al., 2016; Zhou et al., 2015, 2017). The plant regions, sow time and harvest time of the main crops in the different provinces of China, including wheat, maize and rice, were surveyed and summarized. Based on the differences of the farming time, wheat was divided into spring wheat and winter wheat; maize was divided into spring, summer and autumn maize; and rice was divided into early, medium and late rice. The sowing and harvest time of the main crops are shown in Table 2.

Based on the service conditions of the different agricultural machinery throughout the year, we classified the agricultural machinery into four categories. The ten-day uneven coefficients of the emissions were calculated as described in the following sections.

2.5.1. Types needing service throughout the year

Farm transport vehicles, farmland capital construction machinery, farm and sideline products, primary processing machinery and animal husbandry machinery were the types needing service throughout the year. The calculation method of the emission ten-day uneven coefficient for these types are shown in Eq. (5):

$$C_k = \frac{1}{36} \tag{5}$$

where C is the ten-day uneven coefficient; k indicates the k-th working ten-day periods; and 36 represents the total number of the ten-day periods in a year.

Table 2
The sowing and harvest times of the main crops in China.

Crop		Sowing time	Harvest time
Wheat	Spring wheat	Late March to early April	Mid- to late July
	Winter wheat	Mid- to late September to early October	Late May to mid- to late June
Maize	Spring maize	Late April to early May	Late August
	Summer maize	Late May to early June	Mid- to late October
	Autumn maize	Early to mid-July	Late September to early October
Rice	Early rice	Late March to early April	Mid- to late July
	Medium rice	Early April to early May	Mid- to late September
	Late rice	Late June to early July	Early to mid-November

2.5.2. Types needing service during specific periods

These types had specific working periods (e.g., fishing season and cutting period) in a year, including the fishery machinery, timber and fruits machinery, agricultural drainage and irrigation machinery, field managing machine and post-harvest processing machine. The calculation method of the ten-day emission uneven coefficient during the working periods for this type is shown in Eq. (6):

$$C_{i,k} = \frac{1}{N_{i,ten-days}} \quad (6)$$

where C is the ten-day uneven coefficient; k indicates the k-th working ten-day periods; and $N_{i,ten-days}$ is the number of the working ten-day periods for machinery i.

2.5.3. Types needing service influenced by the farming practice and different crops

The service time of these types was influenced by the farming practices and different main crops (e.g., wheat, maize and rice). These types included tilling land machine, equipment for planting and distributing fertilizer and harvesting machine. Eq. (7) shows the calculation method of the emission ten-day uneven coefficient.

$$C_{i,j,k} = \frac{A_{i,j}}{\sum_j A_{i,j}} \times \frac{1}{N_{i,j,ten-days}} \quad (7)$$

where C is the ten-day uneven coefficient; i is the machinery type mentioned above; j indicates the main crop type (i.e., wheat, maize and rice); k indicates the k-th working ten day; A is the area of the mechanization (i.e. machine-plowed, machine-sown or machine-harvested) (NBSC, 2015b); and $N_{i,j,ten-days}$ is the number of the working ten-day periods for the machinery i used for the crop type j.

2.5.4. Type needing complex service

The last type was tractors, which are widely used for farming-related work and transportation. The emission ten-day uneven coefficients were calculated as shown in Eq. (8) for transportation and Eq. (9) for farming-related work.

$$C_{T,k} = \frac{8 \times N_{T,ten-days}}{8 \times N_{T,ten-days} + 24 \times N_{F,ten-days}} \times \frac{1}{N_{T,ten-days}} \quad (8)$$

$$C_{F,i,j,k} = \frac{A_{i,j}}{\sum_i \sum_j A_{i,j}} \times \frac{1}{N_{F,i,j,ten-days}} \quad (9)$$

where C is the ten-day uneven coefficient; i represents the different main crops (i.e. wheat, maize and rice); j is the type of agricultural activity (i.e. plowing, sowing and harvesting); k indicates the k-th working ten-day; A is the area of mechanization; $N_{T,ten-days}$is the number of working ten-days for transportation; $N_{F,ten-days}$ is the number of the ten-day for farming-related work; and $N_{F,i,j,ten-days}$ is the number of the ten-day worked for the activity j of crop i. In addition, 8 and 24 represent the working hours in a transportation day and in a farming work day, respectively. During the busy farming periods, the time for the farming work was tight and the duty was heavy, as a result, we assumed that the tractor worked 24 h every day. During the normal working days for transportation, we supposed that the tractor worked 8 h per day.

3. Results and discussion

3.1. Total emissions in China

Based on the methods described in section 2, the air pollutant emissions of agricultural machinery in mainland China were calculated. Table 3 lists the emissions of the different provinces. In 2014, the total emissions of PM_{10}, $PM_{2.5}$, THC, NOx, CO and SO_2 for the Chinese mainland were 262.69 Gg, 249.25 Gg, 1211.39 Gg, 2192.05 Gg, 1448.16 Gg and 25.14 Gg, respectively. They were approximately 71.9%, 83.0%, 36.4%, 34.5%, 5.2% and 13.0% of the emissions from the on-road vehicles (Lang et al., 2014, 2016), indicating that agricultural machinery was also a non-ignorable source for air pollutants, especially for the PM, THC and NOx emissions. These pollutants were important precursors of the atmospheric $PM_{2.5}$ pollution (Lang et al., 2017), which is the major environmental pollution problem in most areas of China. Consequently, the emissions of agricultural machinery, their environmental implications and their control should be paid attention to, in addition to the motor vehicles. Among the 31 municipalities/provinces, Shandong, Henan, Hebei, Anhui, Hunan Heilongjiang, Inner-Mongolia and Jiangsu are the top eight provinces with the greatest amount of emissions in China. They accounted for 60.0%, 60.0%, 64.8%, 59.7%, 60.2% and 54.0% of the total PM_{10}, $PM_{2.5}$, THC, NOx, CO, and SO_2 emissions, respectively. Conversely, Beijing, Shanghai, Tianjin, Fujian, Hainan, Tibet, Qinghai and Ningxia are the eight provinces/municipalities with the least emissions, accounting for 3.8%, 3.8%, 3.7%, 3.8%, 3.8% and 4.1% of the total PM_{10}, $PM_{2.5}$, THC, NOx, CO, and SO_2 emissions, respectively. These findings were consistent with the development of the agricultural level in these different regions. By using $PM_{2.5}$ as an example, Fig. 2

Table 3
The emissions of the agricultural machinery in the different provinces/municipalities of China in 2014 (Gg).

Area	PM_{10}	$PM_{2.5}$	THC	NO_x	CO	SO_2
Beijing	0.32	0.31	2.27	2.60	1.80	0.0016
Tianjin	1.07	1.02	8.81	8.40	5.96	0.12
Hebei	26.13	24.76	200.04	202.57	142.69	2.16
Shanxi	8.16	7.73	72.11	61.98	44.65	0.62
Inner-Mongolia	10.86	10.31	37.89	92.67	59.95	0.91
Liaoning	6.88	6.52	37.58	56.48	37.98	0.68
Jilin	9.02	8.57	21.19	79.30	50.11	1.08
Heilongjiang	15.36	14.59	27.91	138.25	86.60	1.66
Shanghai	0.15	0.14	0.18	1.45	0.90	0.0035
Jiangsu	10.54	10.00	27.78	95.36	60.51	1.07
Zhejiang	2.66	2.52	10.27	23.10	14.98	0.86
Anhui	16.40	15.56	70.33	138.21	90.84	1.10
Fujian	1.98	1.88	9.37	16.44	10.86	0.29
Jiangxi	4.74	4.50	16.52	39.90	25.72	0.73
Shandong	33.36	31.63	214.61	267.40	183.48	2.80
Henan	33.33	31.62	173.68	273.56	183.28	2.58
Hubei	9.47	9.00	26.58	82.50	52.53	1.01
Hunan	11.73	11.14	32.26	100.28	63.80	1.31
Guangdong	4.36	4.14	14.36	37.02	23.76	0.12
Guangxi	7.62	7.24	25.20	64.64	41.70	0.94
Hainan	1.27	1.21	3.41	10.98	6.98	0.18
Chongqing	2.79	2.65	7.37	23.69	15.06	0.36
Sichuan	7.06	6.71	19.26	60.44	38.43	0.99
Guizhou	4.37	4.14	20.19	35.38	23.22	0.31
Yunnan	7.29	6.92	14.15	63.43	39.77	0.59
Tibet	1.71	1.63	4.46	14.53	9.21	0.19
Shaanxi	5.76	5.46	38.33	45.98	31.66	0.64
Gansu	7.50	7.11	47.54	59.25	40.67	0.90
Qinghai	1.37	1.30	2.77	11.80	7.43	0.08
Ningxia	2.19	2.08	12.99	17.64	11.98	0.16
Xinjiang	7.25	6.89	11.97	66.79	41.66	0.75
Total	262.69	249.25	1211.39	2192.05	1448.16	25.14

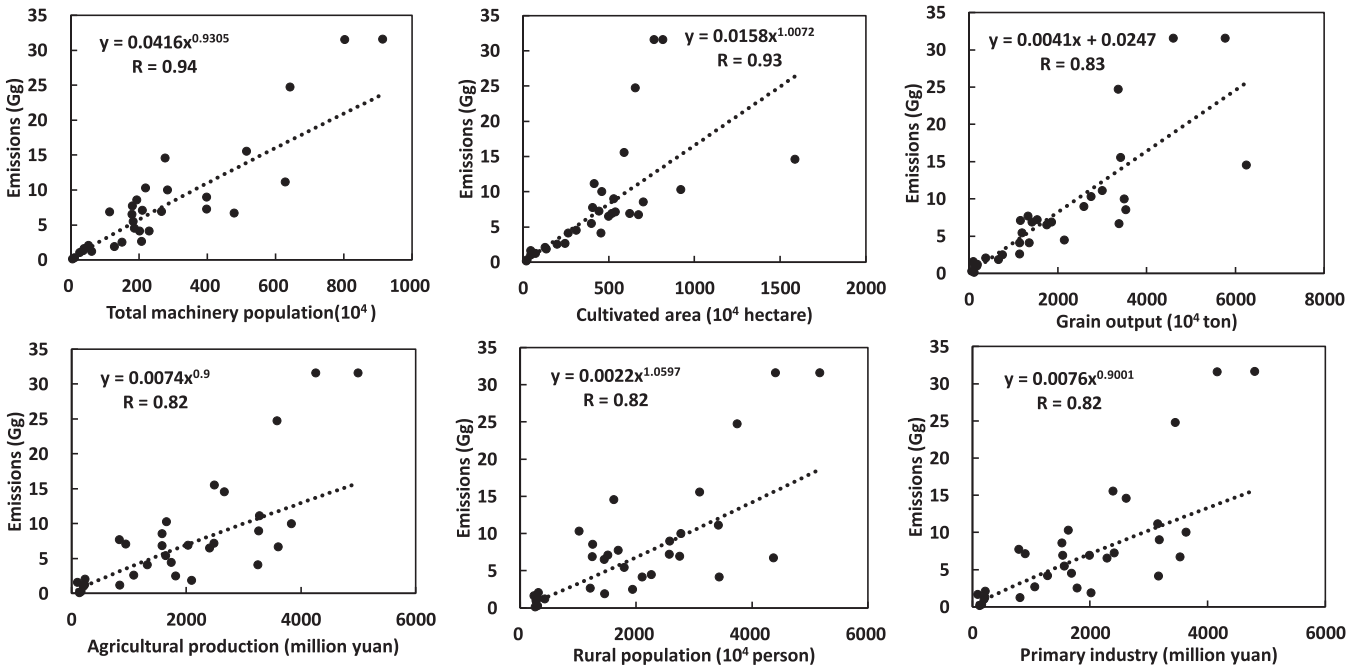

Fig. 2. Correlation between $PM_{2.5}$ emissions and agricultural related data in different provinces.

shows that the emissions had an obvious positive correlation with the cultivated area (R = 0.93), total population (R = 0.90), agricultural production (R = 0.82), grain output (R = 0.87), rural population (R = 0.82) and primary industry (R = 0.82).

Fig. 3 illustrates the contributions of the main agricultural machineries to the different pollutants. It was found that (1) tractors contributed the most to the pollutants, except for THC, and the contribution ratios were 48.9%, 48.9%, 53.6%, 50.2% and 39.9% for PM_{10}, $PM_{2.5}$, NOx, CO and SO_2, respectively; (2) another important contributor to emissions, especially THC emissions, is the farm transport vehicle, and the contribution percentages were 81.8% for THC and 17.4%-24.6% for the other pollutants; and (3) planting machinery also had considerable contributions, with fractions of 4.8%-27.9% for the different pollutants. A larger population of the three agricultural machineries (with a sum percentage of 98.6%) (Fig. 1) and a higher THC emission factor (Table 1) of the farm transport vehicles were the main reasons for the higher contribution ratios. These indicate that the emission control emphasis of the agricultural machinery should be focused on the tractors, farm transport vehicles and planting machinery.

3.2. Spatial distribution of emissions

Based on the methods described in sections 2.2 and 2.4, we estimated the county-level (2836 counties in the 31 municipalities/provinces) agricultural machinery emissions, and distributed them into 1 km × 1 km grids. The emissions maps for all of the species (PM_{10}, $PM_{2.5}$, THC, NO_x, CO, SO_2) presented similar spatial distributions. Thus, we use $PM_{2.5}$ as an example to discuss the spatial distribution characteristics in the following section.

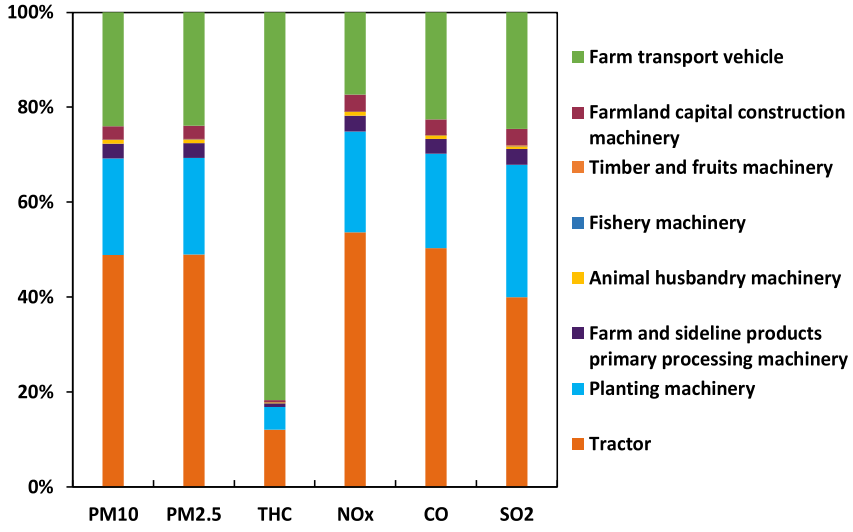

Fig. 3. Contributions of different agricultural machinery types to various pollutants in China in 2014.

3.2.1. Spatial distributions at the county level

In addition to the county-level pollutant emissions, we also calculated the emission intensity per square kilometer (km^2) and per capita (for the rural population) in each county. They are illustrated in Fig. 4. Fig. 4 (a), (c) and (e) show the $PM_{2.5}$ emissions, emissions per unit area, and emissions per capita in different counties, respectively. Fig. 4 (b), (d) and (f) show the corresponding statistical results of the different counties. It can be seen that the counties with the higher emissions are mainly located in the North China Plain (e.g., Hebei, Shandong, Henan, Anhui and Jiangsu province) and the Northeast China Plain (e.g., Heilongjiang and Jilin province) (Fig. 4 (a) and (c)). These plain areas are relatively flat and suitable for agricultural development, and they were also the national core grain-producing areas, with more farmland and agricultural machinery. However, most of the counties with the higher $PM_{2.5}$ emissions per capita were in the provinces of Xinjiang, Xizang and Inner Mongolia (Fig. 4(e)), where the rural population is much lower than the other regions. The statistical results (Fig. 4(b),

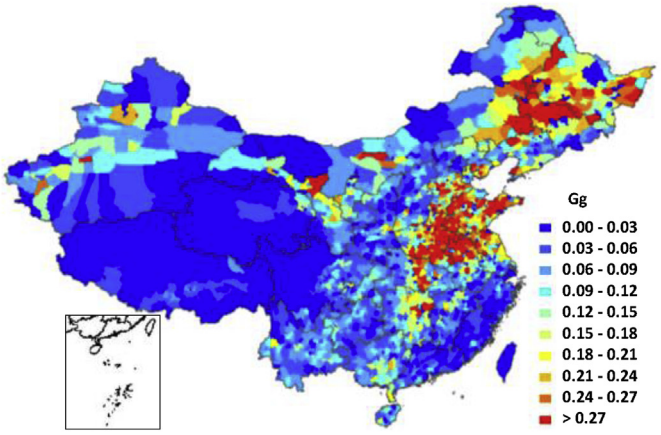

(a) The annual emissions of $PM_{2.5}$ in each county

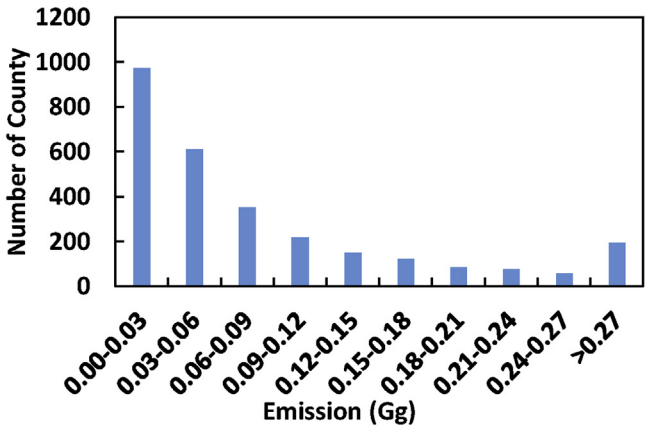

(b) The distribution of county level annual $PM_{2.5}$ emissions

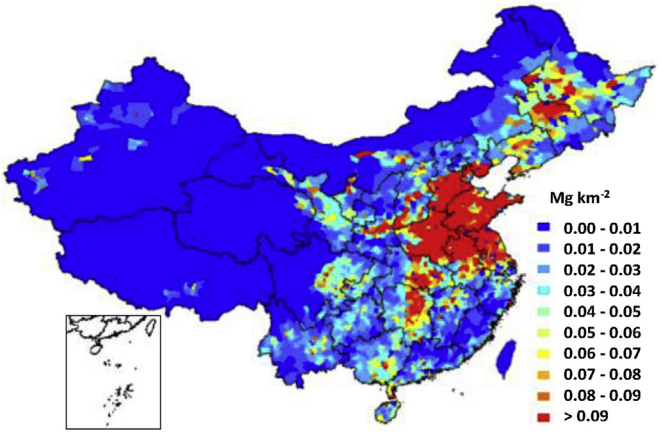

(c) $PM_{2.5}$ emission intensities per unit area

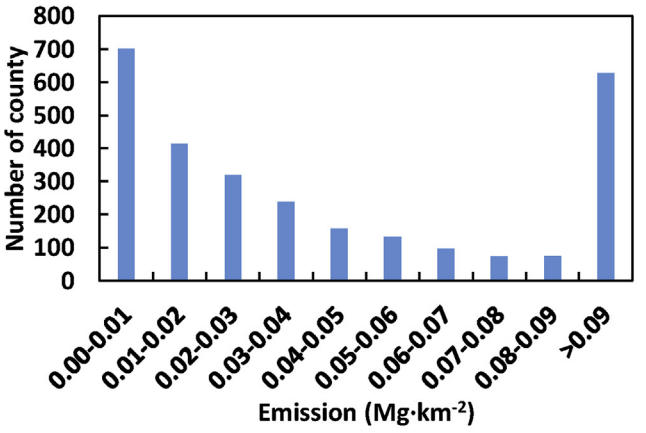

(d) The distribution of emission intensities per unit area

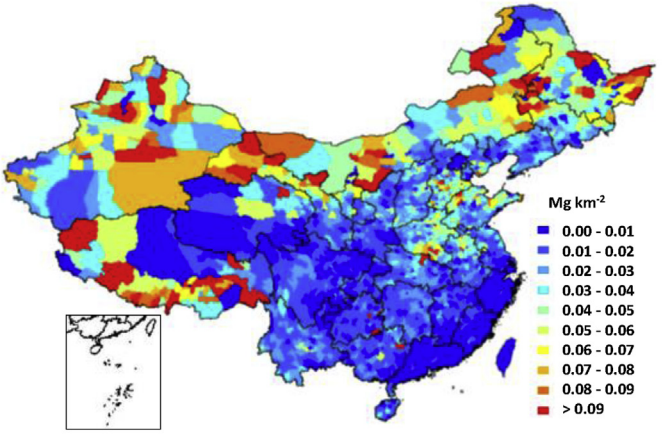

(e) $PM_{2.5}$ emission intensities per capita

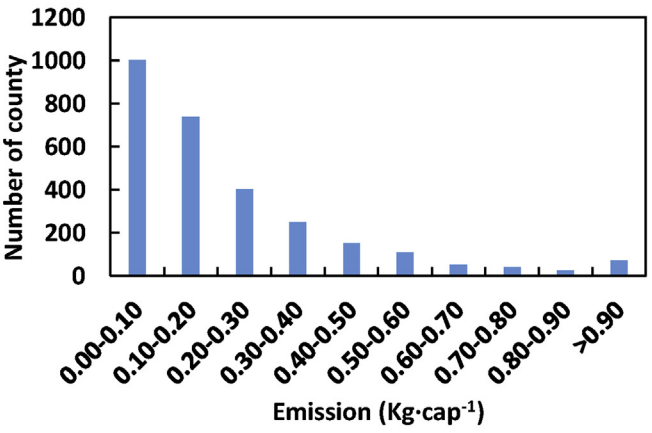

(f) The distribution of emission intensities per capita

Fig. 4. The $PM_{2.5}$ emissions/intensities of agricultural machinery at the county-level resolution.

(d) and (f)) indicate that (1) the county numbers show a general decreasing trend in response to the growth of the emissions/emission intensities and that the counties with emissions of 0.00–0.03 Gg, 0.00–0.01 Mg/km^2 and 0.00–0.10 kg/capita had the largest fractions (34.3%, 24.8% and 35.3%, respectively); (2) the numbers of the counties with $PM_{2.5}$ emissions of more than 0.27 Gg, 0.09 Mg/km^2 and 0.90 kg/capita increased compared to the previous emission ranges (i.e. 0.12–0.27 Gg, 0.01–0.09 Mg/km^2 and 0.60–0.90 kg/capita), and they also had considerable percentages (6.8%, 22.1% and 2.5%, respectively) in the total emissions/intensities.

3.2.2. Gridded emission distribution of agricultural machinery

Based on the methods introduced in section 2.4, the agricultural machinery emissions in the different counties were allocated to the 1 km × 1 km grids by using land cover (i.e. croplands and forests), population (i.e. the rural population) and other proxies. The gridded emissions provide necessary input data for the model simulation. Fig. 5 shows the 1 km × 1 km gridded $PM_{2.5}$ emissions of the agricultural machinery. It can be found that the high agricultural machinery emissions are mainly distributed in the Hebei, Shandong, Henan, and Anhui provinces and so on. These high-emission areas are mainly located in the northeast, north and central-south China, which are the main agricultural areas of the country. They are mainly rural areas with relatively developed agriculture and are characterized by a dense population and richly cultivated areas. However, in parts of the northeast and north-western regions, there are much lower distributed agricultural machinery emissions. These areas are mainly covered with mountains, deserts or forests, and as a result, they have fewer agricultural lands. In addition, in some urban areas (e.g., the Dongcheng and Xicheng districts of Beijing), because there is no cultivated land or agricultural activity, few agricultural machine pollutants were emitted.

3.3. Temporal variation of emissions

Based on the investigated agricultural practice timing, the annual emissions in the different provinces were distributed to the temporal resolution of ten-day periods (i.e. the early, middle and late ten-day periods in each month). The temporal distribution of the different pollutants in China is shown in Fig. 6. It is found that the most significant emission peak was in early October. The

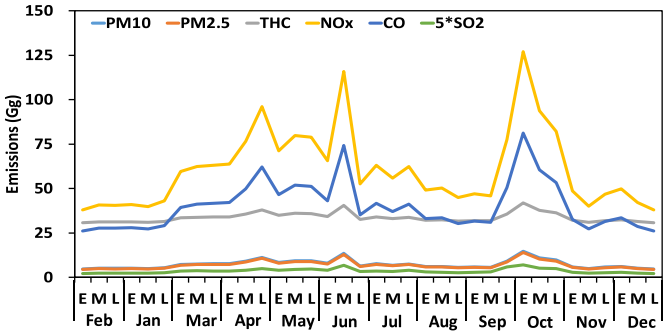

Fig. 6. Ten-day emission variation of the different pollutants in China.

emissions of PM_{10}, $PM_{2.5}$, THC, NO_x, CO and SO_2 accounted for 5.6%, 5.6%, 3.5%, 5.8%, 5.6% and 5.6% of the corresponding annual pollutants emissions, respectively. Other peaks occurred in late April and mid-June. The fraction ranges were 4.3%-5.1%, 4.3%-5.1%, 3.1%-3.3%, 4.4%-5.3%, 4.3%-5.1% and 4.0%-5.4% of the total emissions for the above six pollutants, respectively. Conversely, low emissions appeared in January, February, November, and December. The percentages of the ten-day emissions were mainly around 2%for most of the pollutants in these months.

By using $PM_{2.5}$ as an example pollutant, Fig. 7 shows the ten-day variation of the agricultural machinery emissions in the different provinces/municipalities and the planting regions of the different crops. Table 2 lists the main crops and their planting and harvest periods. It is found that due to the differences of the crop types and planting time, the temporal variation characteristics were different in the 31 provinces/municipalities. Generally, three types of emission distribution characteristics existed: two peaks, three peaks and multiple peaks.

In most of the provinces of northern China and parts of eastern China, including Hebei, Beijing, Tianjin, Shanxi, Inner Mongolia, Liaoning, Heilongjiang, Jilin, Shandong, Henan, Jiangsu, Shanghai, Tibet, Qinghai, Zhejiang and Fujian, there were two significant emission peaks. (1) In North China (Beijing, Tianjin, Hebei, Shanxi, Inner-Mongolia), the temporal distributions were similar, and the significant two peaks appeared in late April to late June and mid-September to early October. The main crops are winter wheat and summer corn in this region (except for Inner-Mongolia).

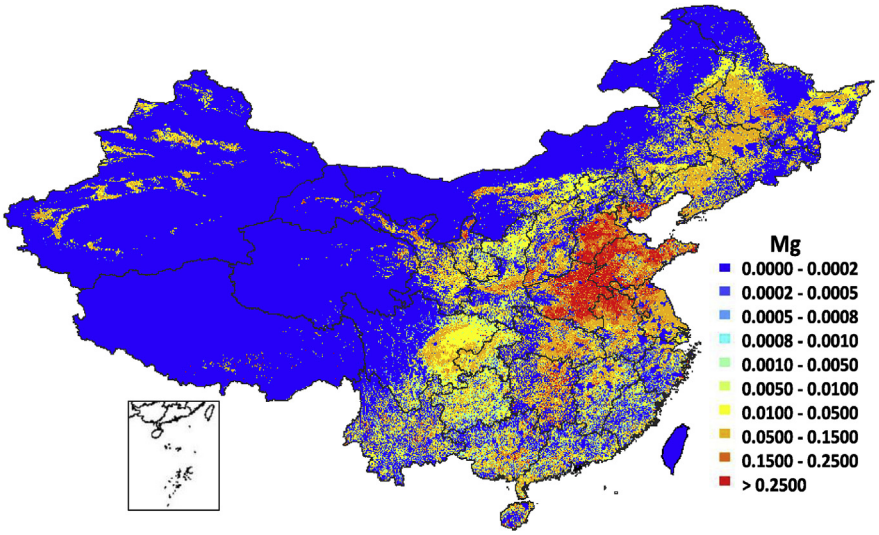

Fig. 5. Gridded (1 km × 1 km) distribution of the $PM_{2.5}$ emissions in mainland China.

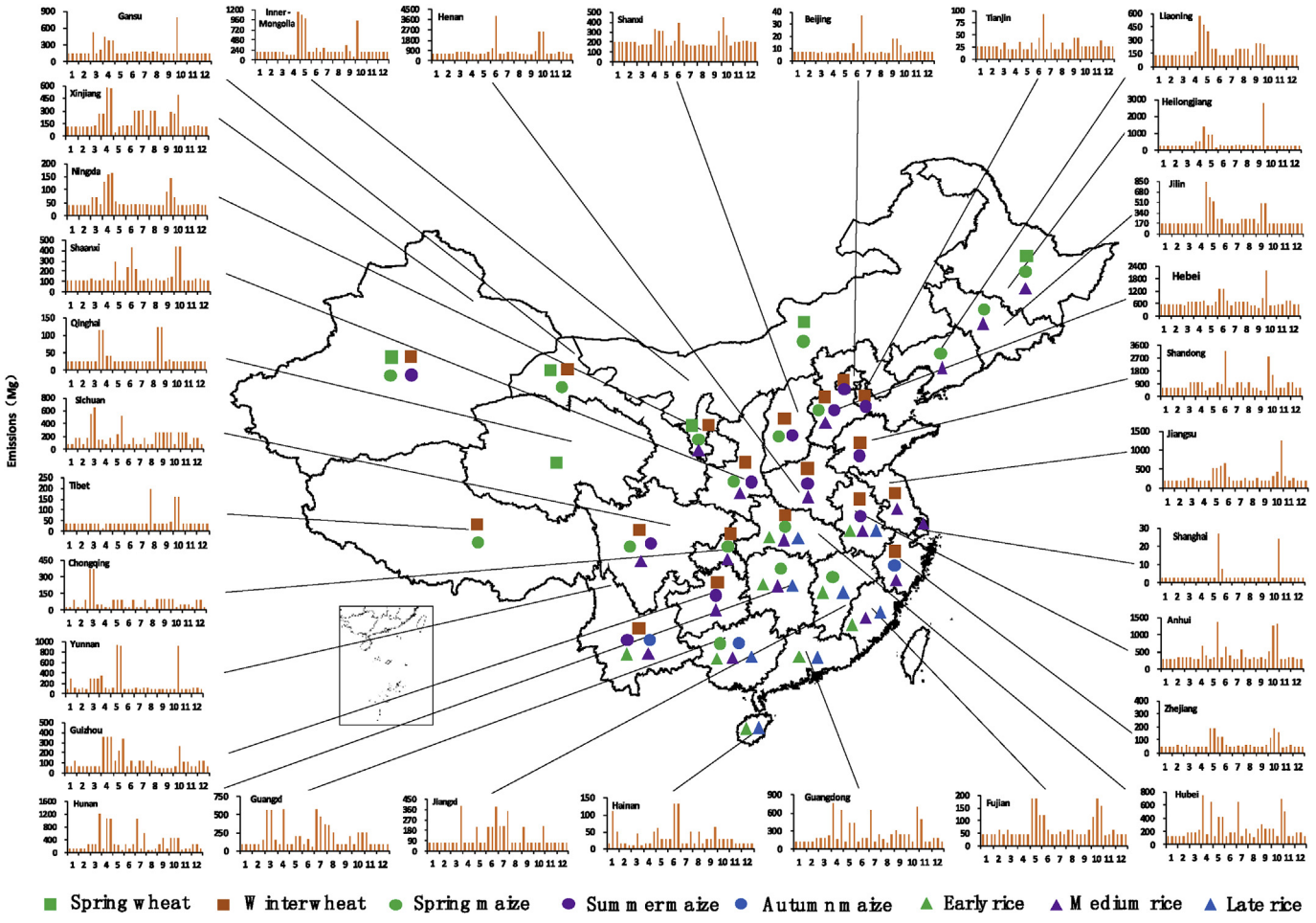

Fig. 7. Plant regions of the main crops and the ten-day variation of the $PM_{2.5}$ emissions in 31 provinces/municipalities.

Particularly, Hebei also planted spring maize and medium rice, and Inner-Mongolia mainly planted the spring- and wheat-maize. The planting times led to the temporal distribution. (2) In Northeast China (including Heilongjiang, Jilin, Liaoning), the higher emissions occurred in late April to mid-May and mid-September to early October. In this region, the climate conditions require that crops are harvested once a year. Spring maize and medium rice are the primary crops in this region, and Heilongjiang also planted spring wheat. (3) Shandong and Henan planted winter wheat and summer maize, causing the peaks in mid-June and early to mid-October. (4) In Jiangsu, the crops were winter wheat and medium rice, which brought the higher emissions in May to early June and late October (5) In Shanghai, the medium rice that was planted contributed to the higher emissions in late May and late October. (6) In Qinghai, the main planted crop was spring wheat, causing obviously higher emissions occurring in late March to early April and late August to early September. (7) In Tibet, winter wheat and spring maize were the main crops, and emissions increased in late August and early to mid-October. (8) The winter wheat, autumn maize and medium rice were planted in Zhejiang, the early, middle, and late rice were planted in Fujian, causing the high peaks in May to early June and October.

In Chongqing, Xinjiang, Gansu, Ningxia and Shaanxi, there were three evident emission peaks. (1) The high emissions in March, May and September in Chongqing were caused by the winter wheat, spring maize and medium rice. (2) In Xinjiang and Gansu, the planted crops were similar; they were spring wheat, winter wheat, spring maize and summer maize (only for Xinjiang), and the higher emissions were distributed around early March to April, late June to mid-August and late September to mid-October. (3) There were four similar types of crops planted in Ningxia and Shaanxi, and they contributed to the higher emissions in early to mid-March, April and mid-September to early October in Ningxia and in early May, June and early to mid-October in Shaanxi.

In other provinces, including Anhui, Hubei, Jiangxi, Guangdong, Hainan, Guangxi, Hunan, Guizhou, Yunnan and Sichuan, there were more emission peaks. Four or five kinds of crops were planted in most of the above provinces (except for Jiangxi, Guangdong and Hainan). Rice was the main crop in all these provinces. In addition, the ripening system in these provinces allowed for two or three harvests a year. The above diversity of crop varieties and the specific cropping systems created the distribution characteristics of the multiple emission peaks.

3.4. Uncertainty analysis

It is inevitable that the estimation of the agricultural machinery emissions contains uncertainties. In this study, the Monte Carlo simulation was adopted to calculate the emission uncertainties. The probability distributions and the coefficients of variations (CVs, the standard deviation divided by the mean) of the parameters (e.g., population, emission factor, load factor, work time, power and so

on, as shown in Eqs. (1)–(3)), must be confirmed first. Considering that (1) the quantitative uncertainty analysis of the agricultural machinery emissions seldom has been conducted, and (2) the emission characteristics were similar to the on-road vehicles, we assumed that the probability distributions and CVs of some parameters used for the agricultural machinery are the same as those for the on-road vehicles (Zhao et al., 2011). Therefore, a normal distribution with a CV of 5% was used for the population (Zhao et al., 2011; Lang et al., 2014, 2016). For the emission factors, the distribution was assumed to be lognormal. The different emission factors had different CVs. The CVs were 47%, 47%, 57%, 33% and 92% for PM_{10}, $PM_{2.5}$, THC, NOx and CO, respectively (Wang et al., 2016). For the load factor, power and work time, there is a lack of statistical information, and in this study, the distributions were assumed to be normal with a CV of 30%. The mileage was assumed to be a normal distribution with a CV of 30%, based on Lang et al.'s (2014) study. In addition, the distributions of the fuel consumption and sulfur content were used as normal with a CV of 16% (Karvosenoja et al., 2008) and 5%, respectively. After the above setting of parameters, 100,000 simulations were performed to calculate the uncertainties of the emissions. The uncertainty ranges (95% confidence intervals) of the total PM_{10}, $PM_{2.5}$, THC, NO_x, CO and SO_2 emissions were −43.9% to 60.9%, −43.6%–60.9%, −71.0%–90.9%, −33.0%–43.3%, −73.2%–93.7%, and −10.7% to 10.8%, respectively.

3.5. Comparison with other studies

The emissions from agricultural machinery in China have been estimated in previous publications (Fan et al., 2011; Jin et al., 2014; Li, 2016; Ning and Li, 2016; Sun et al., 2010; Wang et al., 2016; Wei, 2013; Zhang et al., 2010). We summarized them and made a comparison with the estimated emissions in this study, as shown in Fig. 8. From the perspective of the national emissions, Fig. 8(a) shows that the estimated agricultural machinery emissions in this study were close to Wang et al. (2016) (except for THC) and Ning and Li's (2016) results but are much higher than Li et al. (2016) and Fu et al.'s (2013) calculation results. From the perspectives of the regional emissions, Fig. 8 (b) - (c) shows that our estimations for most of the pollutant emissions in Beijing-Tianjin-Hebei and the Pearl River Delta region were close to those in previous studies (Wei, 2013; Zhang et al., 2010). However, the SO_2 emissions were much lower than those in the above two papers. From the perspective of the province-level emissions, Fig. 8 (d–f) illustrates that the estimated emissions in this paper were generally lower than those calculated by Fan et al. (2011) in Beijing and by Sun et al. (2010) in Jiangsu but were higher than those estimated by Jin et al. (2014) in Tianjin. The above differences may be caused by the following reasons: (1) The calculation methods were different. In this study, the power-based method was used for most of the pollutants, however, most of the rest studies used the fuel consumption-based approach (except for Ning and Li (2016)). (2) The emission factors may come from different sources. (3) There were also differences among the activity data used in the different studies. For example, the average installed engine power used in this study were province-specific, and the analysis indicated that this could reduce the uncertainty of the estimated emissions (section 2.3.1). (4) The types of the agricultural machinery considered were different in the various studies. In this study, most of the agricultural machinery types were considered. As a result, the estimated emissions are higher than those which only considered several types. (5) The use of different base years is also a possible reason, because the population and other calculation parameters varies in different years. For example, the sulfur content of diesel was 350 mg/kg in most of the provinces of mainland China in the base year (2014) of this study, but it was 2000 mg/kg in the base years (2006, 2010) of Zhang et al.'s (2010) and Wei's (2013) studies.

4. Conclusion

In this study, we developed a county-level emission inventory of agricultural machinery in 2014 of mainland China. Six kinds of air pollutants, including PM_{10}, $PM_{2.5}$, THC, NO_x, CO and SO_2, were considered for most of the agricultural machinery in China. The county-level emissions were allocated into a spatial resolution of 1 km × 1 km based on source-specific allocation surrogates. The annual emissions in the different provinces were distributed to a temporal resolution of ten-day periods (i.e. the early, mid- and late ten-day periods of each month), based on a comprehensive

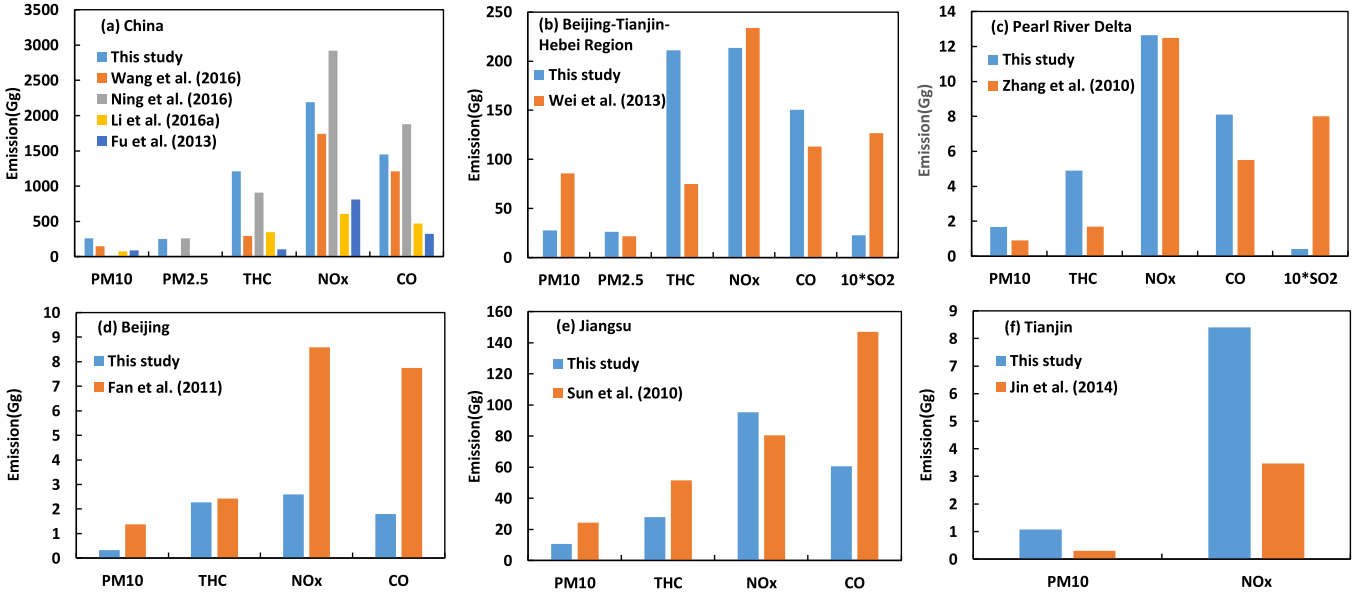

Fig. 8. Comparison between the emissions estimated in this and previous studies.

investigation of the main crop farming timing in China.

The results showed that the total annual emissions of PM_{10}, $PM_{2.5}$, THC, NO_x, CO and SO_2 for the Chinese mainland were 262.69 Gg, 249.25 Gg, 1211.39 Gg, 2192.05 Gg, 1448.16 Gg and 25.14 Gg, respectively. They were approximately 71.9%, 83.0%, 36.4%, 34.5%, 5.2% and 13.0% of the emissions from the on-road vehicles in mainland China. The tractors, farm transport vehicles and planting machinery are the main contributors of the different pollutants. The gridded emission results indicate that the higher agricultural machinery emissions are distributed in the northeast, north and central-south regions of China.

The temporal distribution of the total emissions in China showed that the higher emissions occurred in late April, mid-June and early October. Three types of emission distribution characteristics existed in the different provinces: two peaks, three peaks and multiple peaks. Hebei, Beijing, Tianjin, Shanxi, Inner Mongolia, Liaoning, Heilongjiang, Jilin, Shandong, Henan, Jiangsu, Shanghai, Tibet, Qinghai, Zhejiang and Fujian had two significant emission peaks. Chongqing, Xinjiang, Gansu, Ningxia and Shaanxi had three emission peaks. Anhui, Hubei, Jiangxi, Guangdong, Hainan, Guangxi, Hunan, Guizhou, Yunnan and Sichuan had multiple emission peaks.

The uncertainties of the agricultural machinery pollutant emissions were analyzed by the Monte Carlo simulation. The total uncertainty ranges (95% confidence intervals) were −43.9% to 60.9%, −43.6%–60.9%, −71.0%–90.9%, −33.0%–43.3%, −73.2%–93.7%, and −10.7% to 10.8%, for PM_{10}, $PM_{2.5}$, THC, NO_x, CO and SO_2, respectively.

Acknowledgement

This research was supported by the Natural Sciences Foundation of China (No. 91644110, 51408014 & 51308257) and the New Talent Program of Beijing University of Technology (No. 2017-RX(1)-10). In addition, we greatly appreciated Beijing Municipal Commission of Education and Beijing Municipal Commission of Science and Technology for supporting this work. The authors are grateful to the anonymous reviewers for their insightful comments.

Appendix A. Supplementary data

Supplementary data related to this article can be found at https://doi.org/10.1016/j.jclepro.2018.02.120.

References

Anenberg, S.C., Balakrishnan, K., Jetter, J., Masera, O., Mehta, S., Moss, J., Ramanathan, V., 2013. Cleaner cooking solutions to achieve health, climate, and economic cobenefits. Environ. Sci. Technol. 47 (9), 3944–3952.

Fan, S., Nie, L., Kan, R., Li, X., Yang, T., 2011. Fuel consumption based exhaust emissions estimating from agriculture equipment in Beijing. J. Saf. Environ. 11, 145–148 (in Chinese).

Fu, M., Ding, Y., Yin, H., Ji, Z., Ge, Y., Liang, B., 2013. Characteristics of agricultural tractors emissions under real-world operating cycle. Trans. Chin. Soc. Agric. Eng. 29, 42–48 (in Chinese).

Fu, Y., Tai, A.P.K., 2015. Impact of climate and land cover changes on tropospheric ozone air quality and public health in East Asia between 1980 and 2010. Atmos. Chem. Phys. 15 (17), 10093–10106.

Gu, Y., Yim, S.H.L., 2016. The air quality and health impacts of domestic trans-boundary pollution in various regions of China. Environ. Int. 97, 117–124.

He, J.J., Wu, L., Mao, H.J., Liu, H.L., Jing, B.Y., Yu, Y., Ren, P.P., Feng, C., Liu, X.H., 2016. Development of a vehicle emission inventory with high temporal-spatial resolution based on NRT traffic data and its impact on air pollution in Beijing - Part 2: impact of vehicle emission on urban air quality. Atmos. Chem. Phys. 16 (5), 3171–3184.

Huang, Q., Cheng, S.Y., Perozzi, R.E., Perozzi, E.F., 2012a. Use of a MM5-CAMx-PSAT modeling system to study SO_2 source apportionment in the Beijing metropolitan region. Environ. Model. Assess. 17, 527–538.

Huang, X., Song, Y., Li, M.M., Li, J.F., Huo, Q., Cai, X.H., Zhu, T., Hu, M., Zhang, H.S., 2012b. A high-resolution ammonia emission inventory in China. Global Biogeochem. Cycles 26.

Jin, T., Chen, D., Fu, X., Li, Y., Yi, Z., Lu, K., 2014. Estimation agricultural machinery emissions in Tianjin in 2010 based on fuel consumption. China Environ. Sci. 34, 2148–2152 (in Chinese).

Kapadia, Z.Z., Spracklen, D.V., Arnold, S.R., Borman, D.J., Mann, G.W., Pringle, K.J., Monks, S.A., Reddington, C.L., Benduhn, F., Rap, A., Scott, C.E., Butt, E.W., Yoshioka, M., 2016. Impacts of aviation fuel sulfur content on climate and human health. Atmos. Chem. Phys. 16 (16), 10521–10541.

Karvosenoja, N., Tainio, M., Kupiainen, K., Tuomisto, J.T., Kukkonen, J., Johansson, M., 2008. Evaluation of the emissions and uncertainties of $PM_{2.5}$ originated from vehicular traffic and domestic wood combustion in Finland. Boreal Environ. Res. 13 (5), 465–474.

Kodros, J.K., Scott, C.E., Farina, S.C., Lee, Y.H., L'Orange, C., Volckens, J., Pierce, J.R., 2015. Uncertainties in global aerosols and climate effects due to biofuel emissions. Atmos. Chem. Phys. 15 (15), 8577–8596.

Lang, J.L., Cheng, S.Y., Zhou, Y., Zhang, Y.L., Wang, G., 2014. Air pollutant emissions from on-road vehicles in China, 1999-2011. Sci. Total Environ. 496, 1–10.

Lang, J.L., Zhou, Y., Cheng, S.Y., Zhang, Y.Y., Dong, M., Li, S.Y., Wang, G., Zhang, Y.L., 2016. Unregulated pollutant emissions from on-road vehicles in China, 1999-2014. Sci. Total Environ. 573, 974–984.

Lang, J.L., Zhou, Y., Chen, D.S., Xing, X.F., Wei, L., Wang, X.T., Zhao, N., Zhang, Y.Y., Guo, X.R., Han, L.H., Cheng, S.Y., 2017. Investigating the contribution of shipping emissions to atmospheric $PM_{2.5}$ using a combined source apportionment approach. Environ. Pollut. 229, 557–566.

Li, M.Y., 2016. Research of Mobile Source Inventories. Beijing Institute of Technology (in Chinese).

Li, J., Li, Y.Q., Bo, Y., Xie, S.D., 2016. High-resolution historical emission inventories of crop residue burning in fields in China for the period 1990-2013. Atmos. Environ. 138, 152–161.

Liu, H., Fu, M., Jin, X., Shang, Y., Shindell, D., Faluvegi, G., Shindell, C., He, K., 2016. Health and climate impacts of ocean-going vessels in East Asia. Nature Clim. (Change advance online publication).

Liu, M.M., Huang, Y.N., Ma, Z.W., Jin, Z., Liu, X.Y., Wang, H., Liu, Y., Wang, J.N., Jantunen, M., Bi, J., Kinney, P.L., 2017a. Spatial and temporal trends in the mortality burden of air pollution in China: 2004-2012. Environ. Int. 98, 75–81.

Liu, Y.H., Liao, W.Y., Li, L., Huang, Y.T., Xu, W.J., 2017b. Vehicle emission trends in China's Guangdong Province from 1994 to 2014. Sci. Total Environ. 586, 512–521.

Ministry of Environmental Protection of the People's Republic of China (MEP), 2014. Non-road Mobile Source Emissions Inventory Compiled Technical Guidelines. Available at: http://www.mep.gov.cn/gkml/hbb/bgg/201501/W020150107594587960717.pdf.

Ministry of Agriculture of the People's Republic of China (MOA), 2014. Database of Farming Season. Available at: http://www.zzys.mos.gov.cn/.

National Bureau of Statistics of China (NBSC), 2015a. China Statistical Yearbook. China Statistics Press, Beijing.

National Bureau of Statistics of China (NBSC), 2015b. China Agricultural Machinery Industry Yearbook. China Machine Press, Beijing.

National Bureau of Statistics of China (NBSC), 2015c. China County Statistical Yearbook 2015. China Statistics Press, Beijing.

Ning, Y.L., Li, H., 2016. Estimation for main atmospheric pollutants emissions from mobile sources in China. Chin. J. Environ. Eng. 10, 4435–4444 (in Chinese).

Pan, Y., Li, N., Zheng, J., Yin, S., Li, C., Yang, J., Zhong, L., Chen, D., Deng, S., Wang, S., 2015. Emission inventory and characteristics of anthropogenic air pollutant sources in Guangdong Province. Acta Sci. Circ. 35, 2655–2669 (in Chinese).

Qiu, X.H., Duan, L., Chai, F.H., Wang, S.X., Yu, Q., Wang, S.L., 2016. Deriving high-resolution emission inventory of open biomass burning in China based on satellite observations. Environ. Sci. Technol. 50 (21), 11779–11786.

Ran, Y.H., Li, X., Lu, L., 2010. Evaluation of four remote sensing based land cover products over China. Int. J. Rem. Sens. 31 (2), 391–401.

Sun, J., Lu, G., Liu, S., 2010. Research on status of agricultural pollution in Jiangsu province. Chin. Agri. Mech. 1, 25–27, 31(in Chinese).

Wang, F., Li, Z., Zhang, K.S., Di, B.F., Hu, B.M., 2016. An overview of non-road equipment emissions in China. Atmos. Environ. 132, 283–289.

Wei, X., 2013. Establishment of the non-road mobile source emission inventory in Beijing-Tianjin-Hebei. In: Proceedings of the China Environmental Science Association. China Environmental Science Press, Beijing (in Chinese).

Wu, Y.Y., Gu, B.J., Erisman, J.W., Reis, S., Fang, Y.Y., Lu, X.H., Zhang, X.M., 2016. PM2.5 pollution is substantially affected by ammonia emissions in China. Environ. Pollut. 218, 86–94.

Xie, R., Sabel, C.E., Lu, X., Zhu, W.M., Kan, H.D., Nielsen, C.P., Wang, H.K., 2016. Long-term trend and spatial pattern of $PM_{2.5}$ induced premature mortality in China. Environ. Int. 97, 180–186.

Zhang, L., Zheng, J., Yin, S., Peng, K., Zhong, L., 2010. Development of non-road mobile source emission inventory for the Pearl River Delta region. Environ. Sci. J. Integr. Environ. Res. 31, 886–891 (in Chinese).

Zhang, Q., Jiang, X.J., Tong, D., Davis, S.J., Zhao, H.Y., Geng, G.N., Feng, T., Zheng, B., Lu, Z.F., Streets, D.G., Ni, R.J., Brauer, M., van Donkelaar, A., Martin, R.V., Huo, H., Liu, Z., Pan, D., Kan, H.D., Yan, Y.Y., Lin, J.T., He, K.B., Guan, D.B., 2017. Trans-boundary health impacts of transported global air pollution and international trade. Nature 543 (7647), 705-+.

Zhao, Y., Nielsen, C.P., Lei, Y., McElroy, M.B., Hao, J., 2011. Quantifying the uncertainties of a bottom-up emission inventory of anthropogenic atmospheric pollutants in China. Atmos. Chem. Phys. 11 (5), 2295–2308.

Zheng, B., Zhang, Q., Tong, D., Chen, C.C., Hong, C.P., Li, M., Geng, G.N., Lei, Y., Huo, H.,

He, K.B., 2017. Resolution dependence of uncertainties in gridded emission inventories: a case study in Hebei, China. Atmos. Chem. Phys. 17 (2), 921–933.
Zhou, Y., Cheng, S.Y., Lang, J.L., Chen, D.S., Zhao, B.B., Liu, C., Xu, R., Li, T.T., 2015. A comprehensive ammonia emission inventory with high-resolution and its evaluation in the Beijing-Tianjin-Hebei (BTH) region, China. Atmos. Environ. 106, 305–317.
Zhou, Y., Xing, X., Lang, J., Chen, D., Cheng, S., Wei, L., Wei, X., Liu, C., 2017. A comprehensive biomass burning emission inventory with high spatial and temporal resolution in China. Atmos. Chem. Phys. 17 (4), 2839–2864.